FISEVIER

Contents lists available at ScienceDirect

Results in Control and Optimization

journal homepage: www.elsevier.com/locate/rico



Model-based control of axisymmetric hexarot parallel manipulators



Siamak Pedrammehr ^{a,b,*}, Mohammad Reza Chalak Qazani ^a, Houshyar Asadi ^a, Mir Mohammad Ettefagh ^b, Saeid Nahavandi ^a

- ^a Institute for Intelligent Systems Research and Innovation, IISRI, Deakin University, VIC, Australia
- ^b Faculty of Mechanical Engineering, University of Tabriz, Tabriz, Iran

ARTICLE INFO

Keywords: Hexarot manipulator Model-based control Fuzzy control Dynamics

ABSTRACT

In this research, the control of a hexarot parallel mechanism is investigated. Parallel kinematic simulators or machine tools manipulators suffer from many problems to have a good motion tracking. The inverse kinematics and dynamic formulation that have been developed recently via the Newton-Euler method for a general hexarot mechanism is briefly presented. PID controller and fuzzy incremental controller have been designed and developed as an alternative option of the model-based controller. The efficiency of the model-based controller compared to other controllers has been evaluated. An important contribution of this paper is an appropriate control strategy that improves the tracking performance utilizing the cost effective joint-space sensor. The control scheme development starts with the robust design of the controller-observer of the single actuators. The single objective genetic algorithm is used to tune the controller gains to achieve the least tracking error of joint position. This, moreover, is improved by a centralized feedforward dynamics compensation of the gravity. The validity of the developed model is checked under Simulink environment of MATLAB software, and it is found that the developed model-based controller has the preferable tracking performance rather than the traditional PID and fuzzy incremental controllers The proposed model-based controller is able to decrease the motion tracking error from 55, 20 and 12 to 4 (deg2) for spiral motion compared with PID, FIC and observer-PD, respectively.

1. Introduction

Recently, parallel manipulators have been proposed for the tasks that the serial ones are not capable to perform. Parallel manipulators have high speed and stiffness, and large capacity of load carrying. The most prominent benefit of parallel mechanisms compared to the serial ones is the possibility of assembling active joints on the manipulator base. This, therefore, benefits the faster and more accurate motions. Parallel manipulators, however, suffer from a limited workspace compared to the serial mechanisms. This disadvantageous gap motivates the researchers to invent the new parallel mechanisms in order to solve the workspace problem. A method to extend the workspace size is to employ coaxial actuated arms which have an infinite rotation around their base [1]. These mechanisms also consist the planar manipulators [2]. Hexarot is also a member of axisymmetric coaxial parallel mechanisms that has gained a considerable attention in this research field [1]. Although the various analysis for the hexarots have been reported in the literature [3–11], no modellings exist for the control of these manipulators.

To control the parallel manipulators, the model-based and error-based control schemes are the main strategies [12]. The error-based controller can be modelled by measuring the actuated joints position. PID controllers, which are extremely used in industry, are error-based. In spite of the cost effectivity, practicality and simplicity of the PID controllers, in the case of parallel mechanisms

^{*} Corresponding author at: Institute for Intelligent Systems Research and Innovation, IISRI, Deakin University, VIC, Australia. E-mail address: s.pedrammehr@gmail.com (S. Pedrammehr).

Table 1
The hexarot parallel SBMP details.

DOF	S_i	U_i	R_i	a_{li}	a_{ui}	{P}	{W}
6	Spherical	Universal	Rotational	Lower	Upper	Platform	World
	joint	joint	join	link	link	frame	frame

Table 2The hexarot parallel SBMP kinematic parameters

THE HEAD	The nextroit partition of the nextroit of the									
a_{ui}	a_{li}	h_1	h_2	h_3	h_4	h_5	h_6	s_1	s_2	
0.63	0.728	1.39	1.287	1.335	0.848	0.742	0.303	0.774	0.06	

SI units.

they are not good choice, as they cannot warrant the parallel manipulators high performance dur to their nonlinearity [13]. In order to achieve the lower tracking error, Su et al. [14] investigated the nonlinear PID control according to the joint space. The manipulator adaptive tracking controller with unknown dynamics and kinematics have been introduced by Zhao et al. [15]. These adaptive and nonlinear controls, however, could be employed for lower speed movements. Considering the end-effector rotation and position, the model-based controllers are more complicated but accurate [16]. For this purpose, the forward kinematics should be solved to obtain the desired position of the end effector [17]. Chellal et al. [18] developed a vision-based control of a six degrees of freedom mechanism while measuring the end-effector pose using a motion tracking system. However, instability in dynamic models' absence or using simplified dynamic models by ignoring some parameters, high cost, and computational burden are some disadvantages that affect these controllers. The robust control is the other form of the model-based control method [19]. The sliding mode control is also a form of robust control technique that can deal with external disturbances and uncertain parameters [20,21]. Chattering because of the control actions rapid changing, short life of activators and lack of robustness are the sliding mode control main disadvantages [22]. The linear quadratic Gaussian adaptive controller, adaptive sliding model control and adaptive fuzzy logic control are the other kinds of model-based controls that are available in the literature [23-32]. Pan et al. [33] proposed the highly efficient controller for a fuzzy mechanism with the existence of online learning mechanism. Later, Pan et al. [34] proposed the fuzzy controller for a nonlinear system with DoS attacks via a resilient event-triggered scheme. The proposed resilient eventtriggered strategy can transmit the necessary packets to the controller under non-periodic DoS attacks to reduce the performance loss of the systems and a new security controller subject to the RET scheme and mismatched membership functions is designed to simplify the network control structure under DoS attacks. It is of note that using an appropriate control technique to control the end-effector of hexarot manipulator is considered to fulfil the gap in the literature.

All the previously-proposed controllers for the hexarot did not consider the dynamic model of the mechanism. Due to the complexity of the mechanism and extreme nonlinearity, the traditional controller techniques like PID and FIC would not be able to decrease the motion tracking error in high-frequency motion signals. The model-based control has been developed for a general hexarot manipulator to decrease the complexity of the system for an observer PID to decrease the motion tracking error as much as possible facing high-frequency motion signal in this study. The proposed controller has a high-performance tracking ability as it is necessary in simulation platforms. The observer unit is also considered in the case of measuring the noisy actuator position. The controller gains of the observer-PD and fuzzy incremental controller (FIC) have been tuned by single objective genetic algorithm (GA). MATLAB/Simulink software has been employed to extract models for the PID, FIC and newly proposed controllers in this paper. Finally, the simulation results are provided, discussed and compared for the mentioned controllers.

2. Hexarot manipulator

Hexarot parallel simulation-based motion platform (SBMP) is a connection of six arms between base and the end effector. The arms include upper links a_{ui} (i=1 to 6) and lowers a_{li} (i=1 to 6). The upper links' one side are joined to the base by active rotational joints, and the upper links' other side are joined to the lowers by passive universal joints. The end effector platform is triangular that is connected to the lowers by six passive spherical joints. Fig. 1 shows hexarot SBMP with the details in Tables 1 and 2. For simulator modelling, {W} frame is assumed as the world frame that is at the base of the simulator. In addition, the {P} frame is attached to the end effector. The mechanism has six degrees of freedom (6 DOF) and a large workspace in comparison with traditional parallel manipulators. Hexarot has a good capability of the angular movement that turns this mechanism into high potential simulation platforms. Hexarot can also be used in other fields of engineering such as assembling or welding.

3. Inverse kinematics and dynamic modelling

The inverse position kinematics for a SBMP is to find the active joints' position considering the configuration of the end effector [35–39]. Kinematic Analysis is the basis of other analysis that can be done on the mechanism. The formulation can be utilized in motion planning of mechanism [40-42], the dynamic and vibration modelling of the mechanism [43-45], and its control system development. This section addresses a brief formulation for the kinematics and dynamics of hexarot mechanism that have been developed in [4-6], the new contribution will be addressed in the next sections.

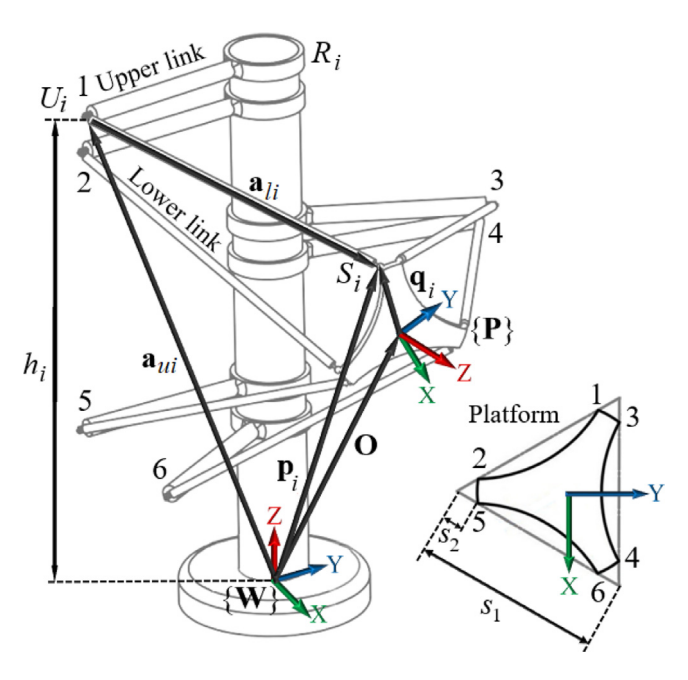


Fig. 1. The hexarot parallel SBMP structure.

According to Fig. 1, and taking \mathbf{O} , p_i , and \mathbf{a}_{ui} as the position vector of the end effector, the spherical joints' position, and the universal joint's position vector, respectively, the lower links' length vector can be formulated as:

$$\mathbf{a}_{li} = \mathbf{O} + \mathbf{p}_i - \mathbf{a}_{ui} \tag{1}$$

The angular position of the upper link, ψ_i , specifies the control system's input signals and can be obtained as:

$$\psi_i = -2 \tan^{-1} \left[\left(b_{i2} \pm \sqrt{-b_{i1}^2 + b_{i2}^2 + b_{i3}^2} \right) / \left(b_{i1} - b_{i3} \right) \right]$$
 (2)

in which b_{i1} , b_{i2} and b_{i3} can be formulated via the end effector configurations [4–6].

 ψ' and ψ'' are the angular velocity and acceleration for the upper links, respectively that are formulated as:

$$\psi' = J \begin{bmatrix} \mathbf{O}' \\ \theta' \end{bmatrix} \tag{3}$$

$$\psi'' = J \begin{bmatrix} O'' \\ \theta'' \end{bmatrix} + J' \begin{bmatrix} O' \\ \theta' \end{bmatrix} \tag{4}$$

 θ' and O' are respectively the end-effector's angular and linear velocities. θ'' and O'' are respectively the time derivatives of θ' and O'. The Jacobian matrix is also shown by J.

To calculate the effect of gravity compensation force for the active joints of the mechanism, the Coriolis, gravity and centripetal forces are considered in the mechanism dynamics. To simplify the dynamic formulation, the effects of friction in active and passive joints are neglected. The flexibility of the links is also negligible.

 \mathbf{F}_{Ui} and \mathbf{M}_{Ui} are the forces and moments applied on the lower links, and defined as:

$$\mathbf{F}_{Ui} = m_U \left(\mathbf{r}_{ii}^{\mathsf{v}} - \mathbf{g} \right) - \mathbf{F}_{Si} \tag{5}$$

$$\mathbf{M}_{Ui} = M_{Ui} \,\mathbf{n}_i \tag{6}$$

where \mathbf{n}_i is the unit vector normal to the universal joint axis, and M_{Ui} is the magnitude of applied moment on the lower links. r_{li} is the length vector of lower links' mass centre, and \mathbf{r}''_{li} is its second derivative. g represents the gravity acceleration. \mathbf{F}_{Si} is also the reaction force exerted from the end effector to the lower links.

 \mathbf{F}_{Ai} and \mathbf{M}_{Ai} are the forces and moments acting on the upper links exerted from the rotational joints, respectively. They can be formulated from the second law of Newton for the link and the moment about the rotational joint, as the following:

$$\mathbf{F}_{Ai} = m_{ij} \left(\mathbf{r}_{ii}^{\prime\prime} - \mathbf{g} \right) + \mathbf{F}_{Ui} \tag{7}$$

$$\mathbf{M}_{Ai} = \mathbf{M}_{Ui} + a_{ui} \mathbf{u}_{ui} \times \mathbf{F}_{Ui} - m_u \mathbf{r}_{ui} \times (\mathbf{r}_{ui}^{"} - \mathbf{g}) + \mathbf{I}_{ui} \psi_i^{"} \mathbf{z} + \psi_i^{'} \mathbf{z} \times \mathbf{I}_{ui} \psi_i^{'} \mathbf{z}$$

$$(8)$$

where m_u and u_{ui} are the upper links' mass and unit vector. I_{ui} are the upper links' inertia tensor. \mathbf{r}''_{ui} are the upper links' mass centre acceleration vector, and it is the second time derivative for \mathbf{r}_{ui} . ψ'_i and ψ''_i are the angular velocities and accelerations for the upper links.

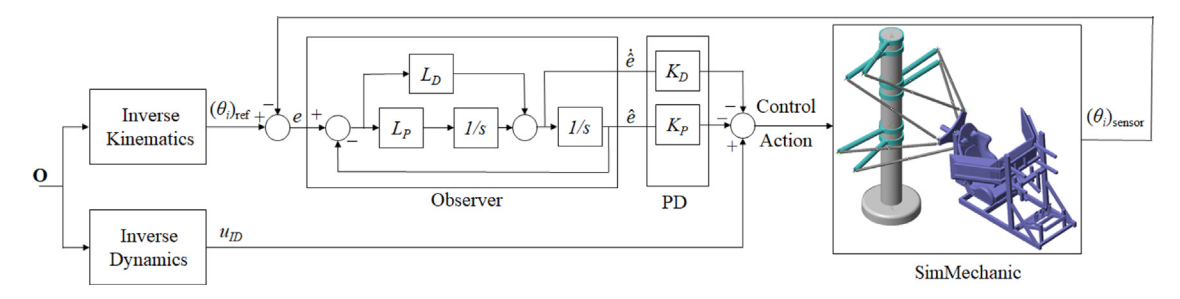


Fig. 2. The developed model-based controller with the observer.

The final actuation torque can be obtained as:

$$\tau_i = \mathbf{M}_{Ai} \cdot \mathbf{z} \tag{9}$$

4. Controller

The proposed model-based controller which is shown in Fig. 2 consisting two main parts. The first part of the controller is composed of the combination of linear observer and PD controller. The feedback observer controller uses the active joints' position error to control the position of the actuators. The second part known as feedforward part is the inverse hexarot mechanism's dynamic model that is utilized to generate the direct control action. It is employed to compensate the effects of gravity towards the end effector of the hexarot parallel mechanism. The control action can be obtained as follows:

$$u = u_{ID} + u_c \tag{10}$$

where u_{ID} is the calculated moment of the active joints that compensates the gravity effects on active joints using Eq. (8). Considering K_P and K_D as PD controller gains, $u_c = -K_D \hat{e}^t - K_P \hat{e}$ is the control effort of PD controller, and \hat{e}^t can be calculated as the following:

$$\hat{e}' = L_P(e - \hat{e}) + L_D(e - \hat{e}) \tag{11}$$

in which L_P and L_D are the proportional and derivative gains for the observer, respectively.

4.1. Robust observer controller

A robust tracking controller with just the joint space tracking measurement is studied in this section. According to Fig. 2 the controller includes a linear observer and a linear feedback part. The observer generates an estimation of the error state from the joint position error. The feedback part uses error state to generate the appropriate control action for the actuators. The controller robustness compared to the common PID controller has been studied by Berghuis [46]. The proposed observer controller is quite useful in the case of noisy actuator sensor measurement. The single objective genetic algorithm has been utilized to obtain the gains for the common PID and proposed observer-PD controller. In the next subsection the genetic algorithm-based optimization of observer-PD controller is explained.

4.2. Genetic algorithm optimizer

To increase the efficiency of the proposed approach, it is critical to select the proper gains for the investigated observer-PD unit. There four indexes including LD, LP, KD and KP that will define inside the GA optimization. The Simulink file of the proposed model-based controller is designed and developed in MATLAB. This Simulink file is defined inside the MATLAB function in order to be called and run based on the selected controller indexes by genetic algorithm. After running the Simulink model by the MATLAB command line the cost function is calculated based on the reported errors of the joints and end effector via the Simulink file. Then, the cost function can be defined as follows:

$$J = \sum_{i=1}^{6} \sum_{k=1}^{N} \left[\left(\theta_i^{\text{ref}}(k) - \theta_i^{\text{sensor}}(k) \right)^2 + \left(X_i^{\text{ref}}(k) - X_i^{\text{sensor}}(k) \right)^2 \right]$$
(12)

where J is the cost function. $\theta_i(k)$ and $X_i(k)$ are also respectively the ith joints and end-effector position at kth time interval. It is possible to define the sensors for the end-effector and joints to recalculate the positions of end-effector, as the simulation model of the hexarot manipulator is developed, i.e. X_i^{sensor} of the mechanism as well as the actuators θ_i^{sensor} . The actual value of these two parameters can be calculated in the inverse kinematics block of the Simulink file. While the input of the inverse kinematics block is X_i^{ref} and the output of the inverse kinematic unit is θ_i^{ref} .

Table 3 presents the GA adjustments and the extracted values. The GA parameters have to be selected adequately to increase the convergence speed and accuracy of the results. The proper selection of the mutation rates and crossover warrants the accuracy

Table 3GA adjustment parameters for FIC controller.

Parameters/Index	Variables number	Population size	Maximum generation	Crossover rate	Mutation function	Function Tolerance	K_P	K_D	L_P	L_D
Value	5	100	20	0.8	Adaptive feasible	10-6	1.62	0.15	0.05	8.15

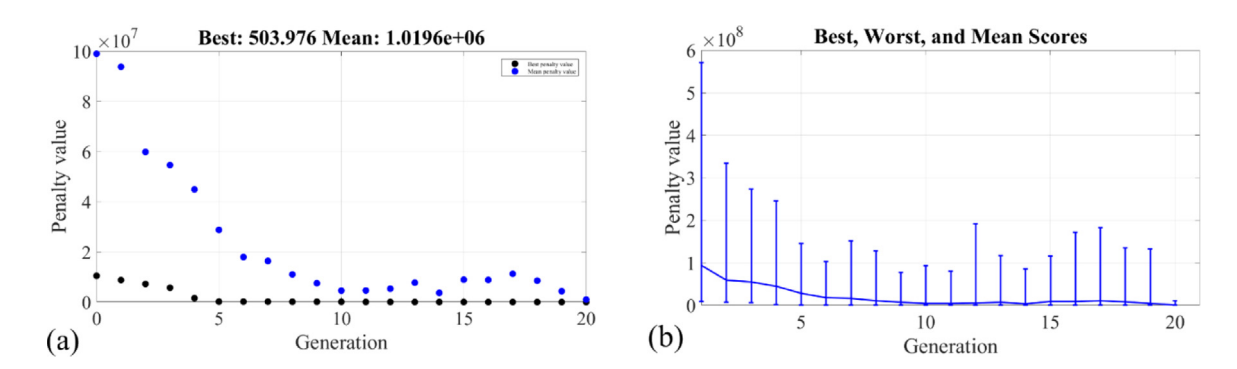


Fig. 3. The developed model-based controller with the observer.

of the GA and obtained results [47,48]. The higher rate of mutation forms the solution missing risk. Moreover, the lower rate of mutation results in becoming stuck in the local optimum position. The population size for this research is assumed to be 80. The lower size of population limits the GA search capability. Vice versa, the higher size of population adds to the optimization time without any considerable improvements in the obtained results [49].

The results demonstrate that the parameters consisting crossover friction, mutation rate, population and generation have proper selection for the current study.

Fig. 3 illustrates the genetic convergence to obtain the best way to minimize the movement tracking error. The GA is run for 20 generations before terminating the optimization process. The best and mean of objective function using the GA are 5.03×102 and 1.02×106 , respectively. It should be noted that the GA is selected as a suitable evolutionary-based optimization method for calculating the optimal PID gains because its fast convergence, which is approved by the presented results in Fig. 3.

4.3. Feedforward inverse dynamic controller

The feedforward part known as u_{ID} . According to the Eq. (8), u_{ID} is added to the control action which is calculated by the observer-PD controller. It enhances the performance tracking of the mechanism which is very important in the case of simulation platform or machine tools to have a high-fidelity motion sensation or the exact tool motion path. To check the tracking error of the proposed controller, the tracking accuracy over a trajectory can be evaluated using square of the active joints position using the following formula:

$$e_{MS} = \frac{1}{6N} \sum_{i=1}^{6} \sum_{k=1}^{N} e_i^2(k) \tag{13}$$

where e_i (k) is the active joints' error at the kth simulation time under the motion path.

4.4. Fuzzy controller

The theory of fuzzy logic has firstly presented by Zadeh [50], and employed in control in early stages [51]. The fuzzy control is one of the applicable approaches for nonlinear systems with inconstant inputs and stochastic behaviours [52]. Fig. 4 illustrates the two-input FIC structure for the under-study manipulator where e(k) and e'(k) are the position of the active joints and the error variation of in time k. e'(k) is obtained as:

$$e'(k) = \frac{e(k) - e(k-1)}{T_s} \tag{14}$$

where e(k-1) and T_s are the error and the sampling time of the active joints' position in the sampling time (k-1).

The output and inputs for FIC have to be normalized inside the discourse of [-1, 1]. To normalize FIC inputs and output inside the interval [-1, 1], the linear gains S_e , S_d and S_u are applied. The single objective GA is used to tune these linear gains to reduce the tracking error of the joint space. Table 4 lists the normalized output and inputs of FIC. Considering the FIC linear gains, the

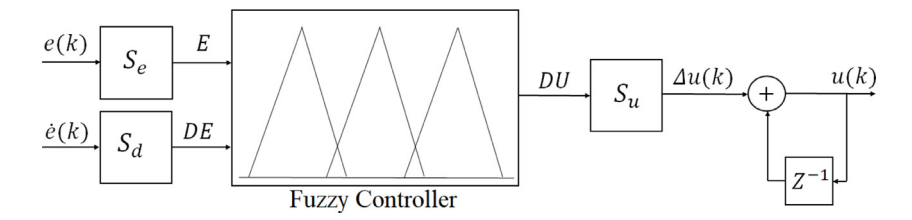


Fig. 4. The two-input FIC structure for a hexarot SBMP.

Table 4
Linear gains of the PID and observer-PD controllers.

	K_P or S_e	K_I	K_D or S_d	L_P or S_u	L_D
PID	[1,10,2,2,10,1] e ⁵	[2.5,1.5,5,5,1.5,2.5] e ³	[5,30,10,10,30,5] e ³	-	_
Observer-PD	[3,30,6,6,30,3] e ⁵	_	[1.5,9,3,3,9,1.5] e ⁴	[1,5,4,4,5,1]	$[2,8,5,5,8,2] e^{-2}$
FIC	1	-	7.6551	31.568	-

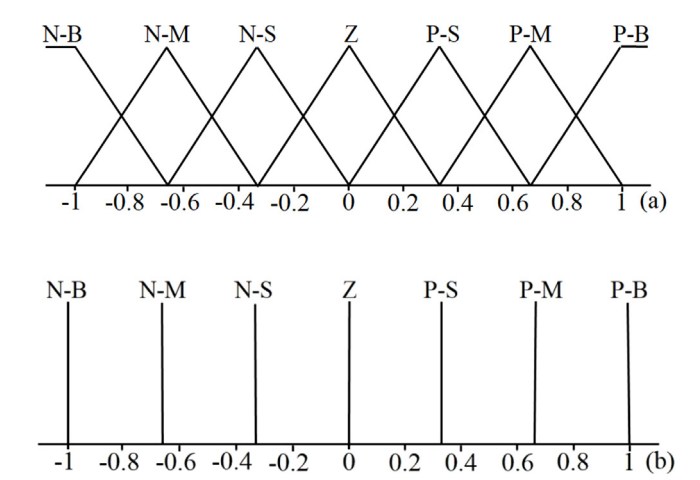


Fig. 5. Memberships: (a) Input weight factor of active joints error and error variation, (b) control action membership functions.

normalized output and inputs of FIC is obtained as:

$$\Delta u(k) = S_u D U \tag{15}$$

$$E = S_{\rho}e(k) \tag{16}$$

$$DE = S_d e'(k) \tag{17}$$

in which $\Delta u(k)$ is the control action change in time k. DU, E and DE are respectively the control action change normalized value, the active joint's position error and the changes in the mentioned error.

To obtain the control action in time k, the recent output has to be added to the previous one. Therefore, the control action for the time k will be as the following:

$$u(k) = u(k-1) + \Delta u(k)$$
 (18)

in which u(k-1) is the FIC control action in the sampling time (k-1).

The Sugeno-type fuzzy blocks and singleton and triangular membership functions are selected to decrease the end effector tracking error as inputs and outputs. For normalized error and error change, the input weight parameters are categorized with seven membership functions such as zero (Z), negative small (N-S), negative medium (N-M), negative big (N-B), positive big (P-B), positive medium (P-M), and positive small (P-S), see Fig. 5(a). The mentioned memberships can warrantee the control action fast rising and better the load disturbance properties. The control action membership function is also divided to seven singelton membership functions negative big (N-B), negative medium (N-M), negative small (N-S), zero (Z), positive small (P-S), positive medium (P-M) and positive big (P-B), see Fig. 5(b).

The Fuzzy logic rules have to be found out after the normalized output and inputs calculation. The rules are established to minimize the mechanism error with description of 91 rules that enlisted in Table 5.

Table 5Fuzzy logic rules to calculate the control action.

DU				E				
DE	N-B	N-M	N-S	Z	P-S	P-M	P-B	
N-B	N-B	N-B	N-B	N-B	N-M	N-S	Z	
N-M	N-B	N-B	N-B	N-M	N-S	Z	P-S	
N-S	N-B	N-B	N-M	N-S	Z	P-S	P-M	
Z	N-B	N-M	N-S	Z	P-S	P-M	P-B	
P-S	N-M	N-S	Z	P-S	P-M	P-B	P-B	
P-M	N-S	Z	P-S	P-M	P-B	P-B	P-B	
P-B	Z	P-S	P-M	P-B	P-B	P-B	P-B	

5. SimMechanics modelling

The Simulink model of the hexarot manipulator considering the PID, FIC and model-based controller are developed and modelled under MATLAB. It includes the motion path generator, kinematics, and dynamics, PID controller, FIC unit, newly proposed modelbased controller and SimMechanics unit. The motion path generator is used to generate the motion signals for the extracted model with controller units. The inverse kinematics and dynamics blocks are designed to calculate the active joints' desired positions and momentum, considering the configuration, velocity and acceleration of the end effector. The extracted positions, velocities and accelerations for the active joints are perceived by the control unit. The PID and FIC controllers of hexarot only receive the active joints' desired positions to calculate their control actions. On the other hand, the observer-PD with combination of the inverse dynamics controller receives the gravity combination moments of the active joints, and the desired position of the active joints to reproduce the control actions for them. The gains for the PID controller, FIC and the developed controller have been chosen according to Table 3 with single objective genetic algorithm. The SimMechanics model being illustrated in Fig. 2 is employed to obtain the mechanism response for the various motion paths during the motion scenarios. It should be noted that the SimMechanic environment of the MATLAB software is employed to developed the most realistic model of the hexarot manipulator compared to the real one in the real world. For developing the SimMechanic model two set of data should be defined including the physical and mechanical data. The physical data is chosen based on the optimal workspace area and the mechanical properties should be chosen based on the real-world application. As a results, the developed model can be equal as the real-world application with less amount of error and higher accuracy.

6. Results and discussions

At first, the hexarot control model with PID, FIC and feedforward model-based controllers are considered to compare the results obtained by the designed control methods without implementing the noise signals to the measurement sensors of the active joints. The sine input signal is assumed to investigate the improvement of the model-based controller for the mentioned manipulator in comparison to the PID and FIC controllers [53]. Three (Hz), high frequency, input signals are exerted to the model in six directions of the end effector to check the end-effector tracking error and the active joints position error.

Fig. 6 illustrates the results of the end-effector tracking error and the active joints position error with six sinusoid signals with various magnitudes: x = 0.4 (m), y = 0.6 (m), z = 0.4 (m), roll=50 (deg), pitch=20 (deg) and yaw=20 (deg).

Considering Fig. 6, the maximum tracking errors with PID controller is 0.18 (mm), 0.24 (mm), 0.16 (mm), 12.5 (degree), 15.5 (degree), and 13.42 (degree) respectively for X, Y, Z Roll, Pitch, and Yaw. The tracking error reduces by using the FIC and model-based controller to 0.02 (mm), 0.015 (mm), 0.025 (mm), 1 (degree), 1 (degree), and 0.5 (degree) for X, Y, Z Roll, Pitch, and Yaw, respectively. It is quite apparent that in the absence of the noise signal, FIC and model-based controller decrease the end-effector tracking error. However, FIC is usually not employed when there is a noisy signal on the joints' position sensor.

The performance for the proposed controller has been investigated to obtain the active joints' positions by implementation of the white noise during two different trajectories shown in Fig. 7. The first motion path is a spiral three dimensional motion about the X axis of the reference frame with the radius of 250 (mm) and longitudinal movement of 300 (mm) that allows about 165 (deg/s) velocity to the active joints. The second motion is the two dimensional quadratic motion with edge length of 200 (mm) that allows 600 (N m) torque to the active joints.

Fig. 8 compares the mentioned tracking error in Eq. (13) for both the motion paths with common PID, FIC, observer-PD and the model-based controllers. It is clear that the observer-PD controller decreases the motion tracking error from 55 to 12 (deg²) during the spiral motion path and from 78 to 52 (deg²) during the quadratic motion path in comparison with the PID controller. FIC also reduces the total tracking error, but it is very sensitive to the disturbances in actuators or sensors.

The proposed model-based control system enhances the tracking performance magnificently from 55 (deg²) for the PID controller to 7 (deg²) during the spiral motion path. It is of note that, to show the influence of the observer-PD controller, the feedforward inverse dynamic model has not been considered.

Fig. 9 demonstrates the end-effector's tracking error for both spiral and quadratic motion paths during the simulation time via four proposed controllers. The magnificent reduction in the end-effector motion tracking error via the model-based controller makes the hexarot parallel manipulator the best choice in the case of the simulation platform either machine tool. This, moreover, proves that FIC controller is not a proper choice in the case of noisy sensor or disturbance compare to the other common controllers.

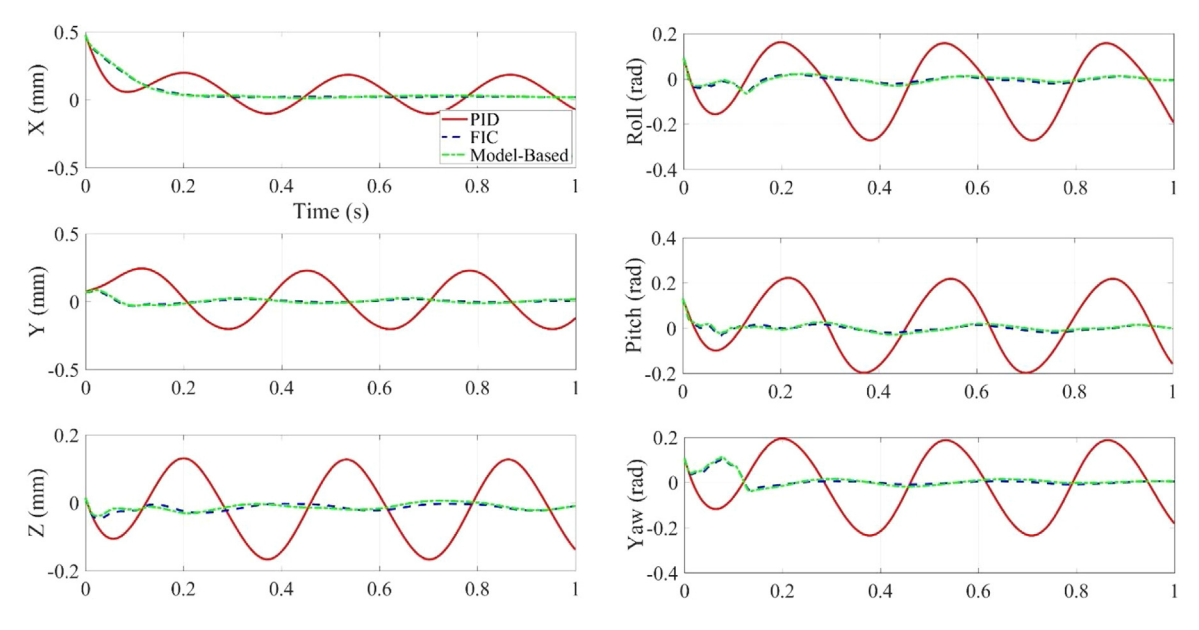


Fig. 6. The tracking errors of the end effector along different directions.

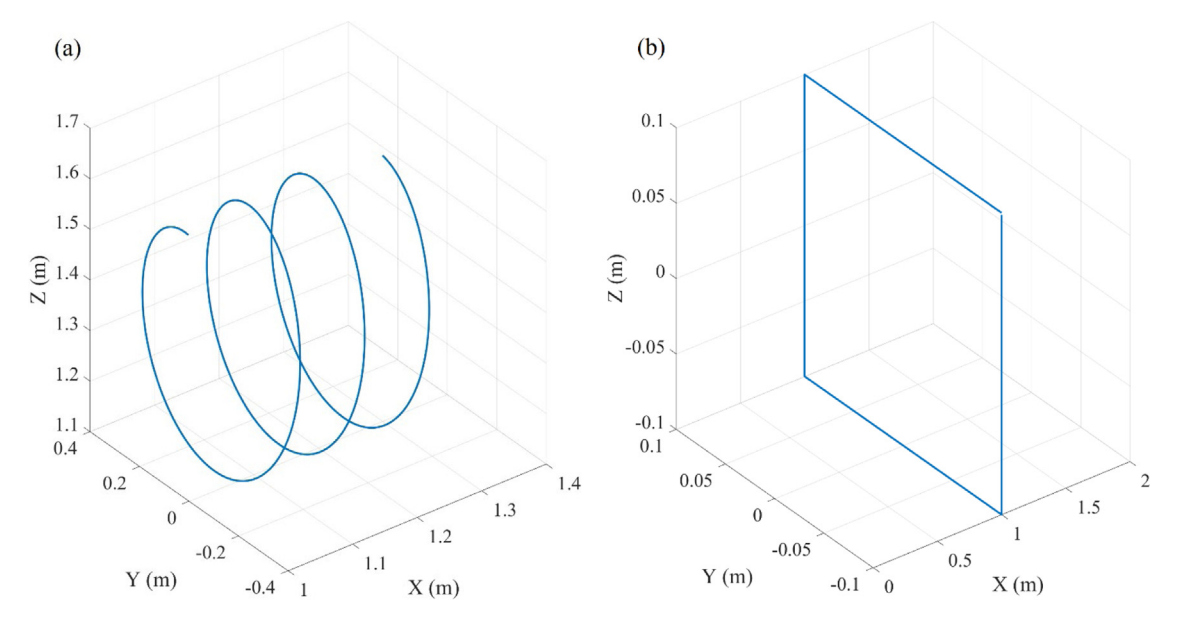


Fig. 7. Motion paths for the investigation of the control performance: (a) spiral motion, (b) quadratic motion.

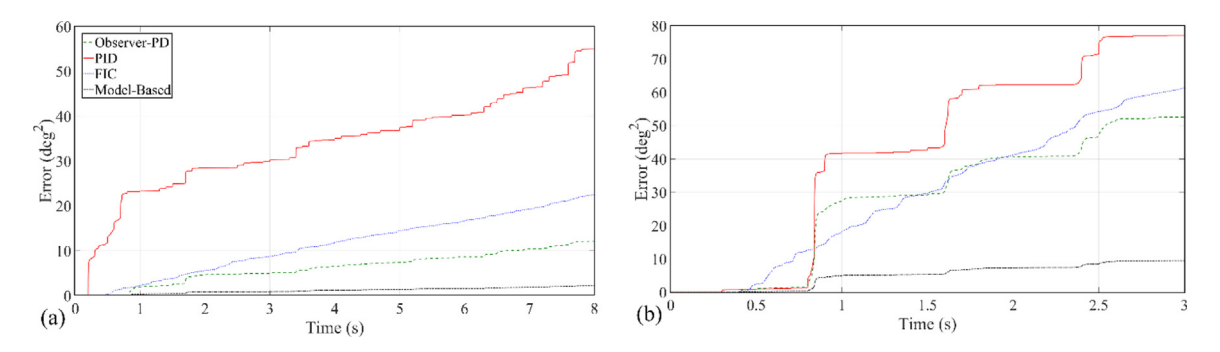


Fig. 8. The motion tracking error of the active joints for PID, observer-PD, and model-based controllers: (a) spiral motion, (b) quadratic motion.

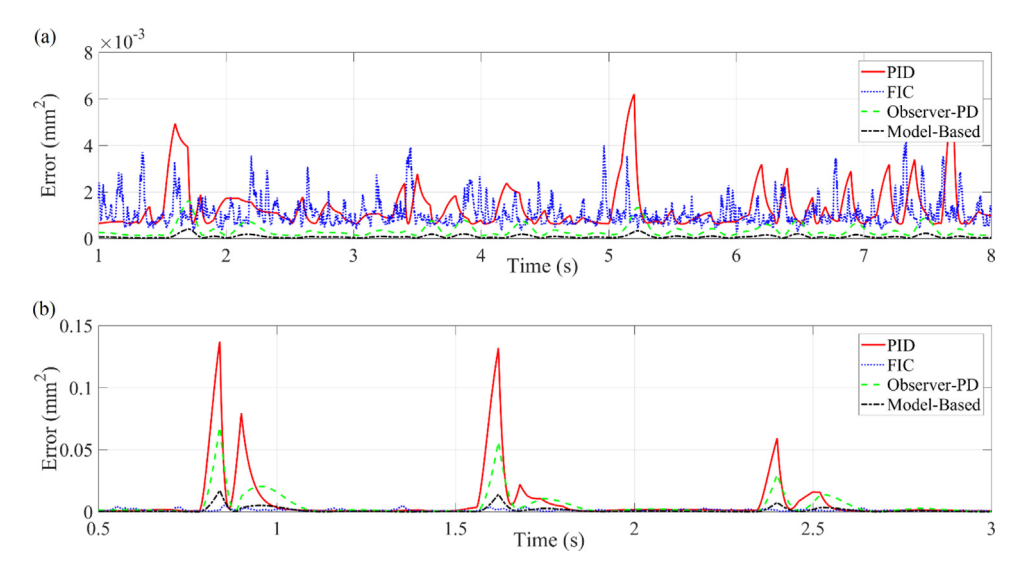


Fig. 9. The end-effector motion tracking error for PID, observer-PD and model-based controllers: (a) spiral motion, (b) quadratic motion.

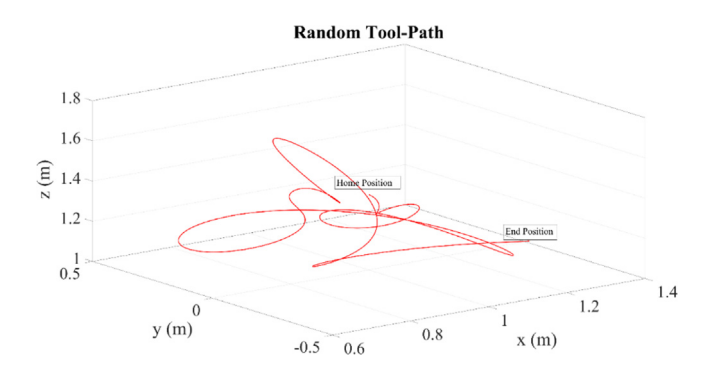


Fig. 10. The randomly free-form regenerated motion signal for end-effector of the hexarot platform to investigated the efficiency of proposed model-based controller in comparison with those of PID, FIC and observer-PD.

At the final validation stage of the proposed model-based controller technique in comparison with other three investigated methods including PID, FIC and observer-PD, the free form randomly regenerated tool-path is tested on the proposed hexarot Simulink platform to show the higher performance of the proposed method. Fig. 10 shows the randomly real-time regenerated tool-path using the whit noise signal with combination of butterworth filter in order to smoothen the regenerated path. The low-path 3 cut-off frequency signal is assigned for a butterworth. It should be noted that the order of the filter remains 8 as the default value of MATLAB software. The start position and end position of the end-effector are shown in Fig. 10. The free-form randomly motion is last for 10 s in order to calculate the motion tracking errors of the end-effector during the action.

Lastly, Fig. 11 shows the motion tracking error of the end-effector during the 15 seconds of the motion following the free-form tool path of Fig. 10. As it is shown in Fig. 11, the model-based controller is able to decrease the motion tracking error significantly higher than other three investigated methods. In this subject, the PID is the worst option for a hexarot high-G simulator facing high-frequency motion signals. FIC has difficulty in adjusting the motion at the beginning but it is able to reach the better result than PID and observer-PD in long-term motion signals. However, the model-based controller is able to reduce the end-effector motion tracking error more than one-third compared to other methods.

The proposed model-based controller for the hexarot manipulator enhances the tracking performance of this mechanism in comparison with the traditional PID controller and artificial intelligence FIC controller. It could also be more useful when there is a noisy signal with the measurement systems of the active joints' positions. The proposed controller does not require high-cost sensors to track the end-effector motion as well. The proposed controller is suitable to be used in the motion simulation platform and machine tool applications of hexarots.

7. Conclusions

In this study, hexarot 6-DOF manipulator as a motion simulation platform or a machine tool with model-based controller was proposed. PID is almost common control method for the industrial usage, as it is easy tuning and cost efficient, however, it mostly

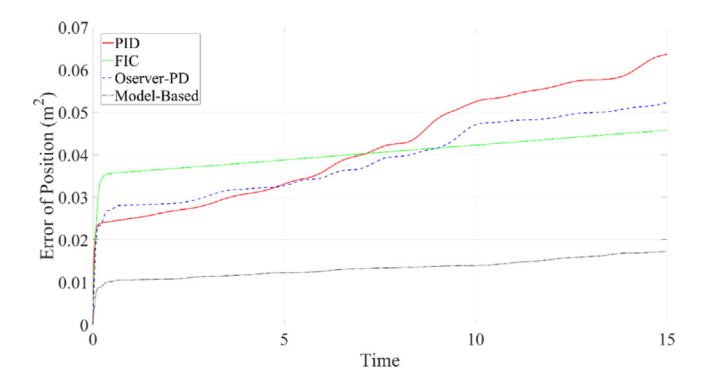


Fig. 11. The motion tracking error of the end-effector using PID, FIC, observer-PD, and model-based controllers.

cannot be able to reach the best accuracy in motion. The low tracking error is of importance in improvement of the motion fidelity and surface roughness respectively in the motion platforms and machine tools. The hexarot mechanism has a high available workspace boundaries, and more available end-effector angular displacement. The observer-PD controller was developed and applied to decrease the tracking error and the joints' position error inside the manipulator control unit. The feedforward inverse dynamic unit was modelled and added to the control unit to produce the gravity compensation moment of the active force independently. The feedforward inverse dynamic unit is able to calculate the joints actions in order to decrease the nonlinearity of the mechanism which has been handled via the observer-PID. This, however, is the main reason of the performance improvement using the proposed method compared to the previous PID, FIC and observer-PID methods. All the gains of the controller were tuned by single objective GA in MATLAB software to reach the better performance motion tracking. The improvement of the observer-PD controller compared to PID and FIC controllers was approved by implementing two specific motion paths. The magnificent reduction of the motion tracking error was recorded by activating the model-based unit of the controller. Finally, the efficiency of the proposed control method in industrial cases of the manipulator was proven.

Declaration of competing interest

The authors declare that they have no known competing financial interests or personal relationships that could have appeared to influence the work reported in this paper.

References

- [1] Isaksson M, Brogårdh T, Watson M, Nahavandi S, Crothers P. The Octahedral Hexarot—A novel 6-DOF parallel manipulator. Mech Mach Theory 2012;55:91–102.
- [2] Pedrammehr S. Dynamic modelling of hexarot parallel mechanisms for design and development (Ph.D. thesis), Australia: Deakin University; 2018.
- [3] Pedrammehr S, Qazani MRC, Abdi H, Nahavandi S. Mathematical modelling of linear motion error for hexarot parallel manipulators. Appl Math Model 2016;40:942-54.
- [4] Pedrammehr S, Danaei B, Abdi H, Masuleh M Taleh, Nahavandi S. Dynamic analysis of Hexarot: axissymmetric parallel manipulator. Robotica 2018;36:225–40.
- [5] Pedrammehr S, Najdovski Z, Abdi H, Nahavandi S. Design methodology for a hexarot-based centrifugal high-G simulator. In: 2017 IEEE international conference on systems, man, and cybernetics SMC. 2017, (3255) 5-8-3260.
- [6] Pedrammehr S, Nahayandi S, Abdi H, Evaluation of inverse dynamics of hexarot-based centrifugal simulators. Int J Dvn Control 2018:6:1505-15.
- [7] Pedrammehr S, Nahavandi S, Abdi H. Closed-form dynamics of hexarot parallel manipulator by means of the principle of virtual work. Acta Mech Sin 2018;34:883–95.
- [8] Pedrammehr S, Qazani MRC, Nahavandi S. A novel axis symmetric parallel mechanism with coaxial actuated arms. In: 2018 4th International conference on control, automation and robotics. IEEE; 2018, p. 476–80.
- [9] Pedrammehr S, Qazani MRC, Asadi H, Nahavandi S. Kinematic manipulability analysis of hexarot simulators. In: The 20th IEEE international conference on industrial technology IEEE-ICIT 2019, Melbourne, Australia, February 13-15. 2019.
- [10] Pedrammehr S, Nahavandi S, Asadi H. The forced vibration analysis of hexarot parallel mechanisms. In: The 20th IEEE international conference on industrial technology IEEE-ICIT 2019, Melbourne, Australia, February 13-15. 2019.
- [11] Pedrammehr S, Qazani MRC, Nahavandi S, Asadi H. Control system development of a hexarot-based high-G centrifugal simulator. In: The 20th IEEE international conference on industrial technology IEEE-ICIT 2019, Melbourne, Australia, February 13-15. 2019.
- [12] Khosravi MA, Taghirad HD. Dynamic modeling and control of parallel robots with elastic cables: singular perturbation approach. IEEE Trans Robot 2014;30:694–704.
- [13] Kim HS, Cho YM, Lee K-I. Robust nonlinear task space control for 6 DOF parallel manipulator. Automatica 2005;41:1591-600.
- [14] Su Y, Duan B, Zheng C. Nonlinear PID control of a six-DOF parallel manipulator. In: IEEE proceedings-control theory and applications. Vol. 151. 2004, p. 95–102.
- [15] Zhao D, Li S, Zhu Q. Adaptive synchronised tracking control for multiple robotic manipulators with uncertain kinematics and dynamics. Internat J Systems Sci 2016;47:791–804.
- [16] Cazalilla J, Vallés M, Valera Á, Mata V, Díaz-Rodríguez M. Hybrid force/position control for a 3-DOF 1T2R parallel robot: Implementation, simulations and experiments. Mech Based Des Struct Mach 2016;44:16–31.

- [17] Merlet J-P, Alexandre-dit Sandretto J. The forward kinematics of cable-driven parallel robots with sagging cables. In: Cable-driven parallel robots. Springer; 2015. p. 3–15.
- [18] Chellal R, Cuvillon L, Laroche E. Model identification and vision-based H∞ position control of 6-DoF cable-driven parallel robots. Internat J Control 2017:90:684-701.
- [19] Grewal KS, Dixon R, Pearson J. LQG controller design applied to a pneumatic stewart-gough platform. Int J Autom Comput 2012;9:45-53.
- [20] Chen S-H, Fu L-C. Output feedback sliding mode control for a Stewart platform with a nonlinear observer-based forward kinematics solution. IEEE Trans Control Syst Technol 2013;21:176–85.
- [21] Guo H, Liu Y, Liu G, Li H. Cascade control of a hydraulically driven 6-DOF parallel robot manipulator based on a sliding mode. Control Eng Pract 2008;16:1055–68.
- 22] Koekebakker SH. Model based control of a flight simulator motion system. 2001, uuid:eccd2fa5-e4f1-43ff-b074-3d6245fa24b9.
- [23] Li Y, Tong S, Li T. Composite adaptive fuzzy output feedback control design for uncertain nonlinear strict-feedback systems with input saturation. IEEE Trans Cybern 2015;45:2299–308.
- [24] Qazani MRC, Asadi H, Pedrammehr S, Nahavandi S. Performance analysis and dexterity monitoring of hexapod-based simulator. In: 2018 4th International conference on control, automation and robotics. IEEE; 2018, p. 226–31.
- [25] Shen T. Special issue on model-based optimal control theory and technology in automotive control. Control Theory Technol 2017;15:81-2.
- [26] Asadi H, Mohamed S, Lim CP, Nahavandi S. Robust optimal motion cueing algorithm based on the linear quadratic regulator method and a genetic algorithm. IEEE Trans Syst Man Cybern Syst 2017;47:238–54.
- [27] Zhao Q, Wang N, Spencer Jr BF. Adaptive position tracking control of electro-hydraulic six-degree-of-freedom driving simulator subject to perturbation. Simulation 2015;91:265–75.
- [28] Mohammadi A, Asadi H, Mohamed S, Nelson K, Nahavandi S. Optimizing model predictive control horizons using genetic algorithm for motion cueing algorithm. Expert Syst Appl 2018;92:73–81.
- [29] Asadi H, Mohamed S, Nelson K, Nahavandi S. A linear quadratic optimal motion cueing algorithm based on human perception. In: ACRA 2014: proceedings of australasian conference on robotics and automation. Australian Robotics and Automation Association; 2014, p. 1–9.
- [30] El-Ghazaly G, Gouttefarde M, Creuze V. Adaptive terminal sliding mode control of a redundantly-actuated cable-driven parallel manipulator: cogiro. In: Cable-driven parallel robots. Springer; 2015, p. 179–200.
- [31] Mohammadi A, Asadi H, Mohamed S, Nelson K, Nahavandi S. MPC-based motion cueing algorithm with short prediction horizon using exponential weighting. In: 2016 IEEE international conference on systems, man, and cybernetics SMC. IEEE; 2016, 000521-000526.
- [32] Mohammadi A, Asadi H, Mohamed S, Nelson K, Nahavandi S. Future reference prediction in model predictive control based driving simulators. In:

 Australasian conference on robotics and automation. 2016.
- [33] Pan Y, Li Q, Liang H, Lam HK. A novel mixed control approach for fuzzy systems via membership functions online learning policy. IEEE Trans Fuzzy Syst 2021. http://dx.doi.org/10.1109/TFUZZ.2021.3130201.
- [34] Pan Y, Wu Y, Lam HK. Security-based fuzzy control for nonlinear networked control systems with DoS attacks via a resilient event-triggered scheme. IEEE Trans Fuzzy Syst 2022. http://dx.doi.org/10.1109/TFUZZ.2022.3148875.
- [35] Pedrammehr S, Mahboubkhah M, Pakzad S. An improved solution to the inverse dynamics of the general Stewart platform. In: 2011 IEEE international conference on mechatronics. 2011, p. 392–7.
- [36] Tajari MJ, Pedrammehr S, Qazani MRC, Nategh MJ. The effects of joint clearance on the kinematic error of the hexapod tables. In: 2017 5th RSI international conference on robotics and mechatronics. 2017, p. 39–44.
- [37] Pedrammehr S, Mahboubkhah M, Khani N. Improved dynamic equations for the generally configured Stewart platform manipulator. J Mech Sci Technol 2012;26:711-21.
- [38] Pedrammehr S. Investigation of factors influential on the dynamic features of machinetools' hexapod table. In: 2nd International conference on acoustics and vibration ISAV2012, Vol. 2, 2012, p. 176
- [39] Rahmani A, Ghanbari A, Pedrammehr S. Kinematic analysis for hybrid 2 (6 UPU) manipulator by wavelet neural network. Adv Mater Res 2014;1016;726–30.
- [40] Qazani MRC, Pedrammehr S, Nategh MJ. A study on motion of machine tools' hexapod table on freeform surfaces with circular interpolation. Int J Adv Manuf Technol 2014;75:1763–71.
- [41] Asadi H, Mohamed S, Zadeh D Rahim, Nahavandi S. Optimisation of nonlinear motion cueing algorithm based on genetic algorithm. Veh Syst Dyn 2015;3:526-45.
- [42] Qazani MRC, Pedrammehr S, Nategh MJ. An investigation on the motion error of machine tools' hexapod table. Int J Precis Eng Man 2018;19:463-71.
- [43] Pedrammehr S, Mahboubkhah M, Qazani MRC, Rahmani A, Pakzad S. Forced vibration analysis of milling machine's hexapod table under machining forces. Strojniskivestnik J Mech Eng 2014;60:158–71.
- [44] Pedrammehr S, Mahboubkhah M, Khani N. A study on vibration of Stewart platform-based machine tool table. Int J Adv Manuf Technol 2013;65:991–1007.
- [45] Pedrammehr S, Mahboubkhah M, Khani N. Natural frequencies and mode shapes for vibrations of machine tools' hexapod table. In: 1st International conference on acoustics and vibration ISAV2011. Vol. 1. 2011, p. 1–8.
- [46] Berghuis H, Nijmeijer H. Robust control of robots via linear estimated state feedback. IEEE Trans Automat Control 1994;39:2159-62.
- [47] Lin W-Y, Lee W-Y, Hong T-P. Adapting crossover and mutation rates in genetic algorithms. J Inf Sci Eng 2003;19:889-903.
- [48] Ochoa G, Harvey I, Buxton H. On recombination and optimal mutation rates. In: Proceedings of the genetic and evolutionary computation conference, 1: citeseer. 1999, p. 488–95.
- [49] Roeva O, Fidanova S, Paprzycki M. Population size influence on the genetic and ant algorithms performance in case of cultivation process modeling. In: Recent advances in computational optimization. Springer; 2015, p. 107–20.
- [50] Zadeh LA. Fuzzy logic: advanced concepts and structures. IEEE Educational Activities Department; 1992.
- [51] Zhang M, Zhang H. Robust adaptive fuzzy control scheme for nonlinear system with uncertainty. J Control Theory Appl 2006;4:209–16.
- [52] Wang M, Qiu J, Feng G. Event-triggered state estimation for T-S fuzzy affine systems based on piecewise Lyapunov-Krasovskii functionals. Control Theory Technol 2019;17:99–111.
- [53] Liu G, Qu Z, Liu X, Han J. Tracking performance improvements of an electrohydraulic Gough-Stewart platform using a fuzzy incremental controller. Ind Robot Int J 2014;41:225–35.